Communication

Synthesis of Sparse Linear Arrays via Low-Rank Hankel Matrix Completion

Xuejing Zhang and Tianyuan Gu

Abstract— In this communication, we propose a method to synthesize sparse linear arrays using low-rank Hankle matrix completion. With the given metrics (e.g., peak sidelobe level (PSL), mainlobe width) of the desired beampattern, we synthesize a sparse linear array directly by designing a low-rank Hankel matrix under appropriate constraints. A low-rank matrix completion problem is formulated with Hankle structure constraint, and an effective solver is presented using log-det heuristic. Different from existing work that requires reference array and reference beampattern, our method synthesizes sparse linear arrays directly according to the desired beampattern metrics. In this way, our method is more flexible and avoids the selection of reference array/beampattern. Moreover, due to maintaining the Hankel structure, the proposed method can achieve more accurate estimation on element positions. In addition, the proposed method can be easily extended and applied to various sparse array synthesis scenarios. Representative simulations are conducted to validate the effectiveness and superiority of the proposed method. It is shown that the proposed method synthesizes desired beampatterns with fewer antenna elements, compared with existing work.

Index Terms— Focused/shaped beampattern, log-det heuristic, low-rank Hankel matrix completion, sparse array synthesis.

I. INTRODUCTION

Sparse array refers to a type of antenna array where the elements are not evenly spaced or distributed [1]. In contrast to a uniform linear array (ULA) or a planar array with regular spacing between elements, a sparse array deliberately varies the spacing between its elements. This nonuniform spacing offers a cost-effective solution for systems requiring large apertures with fewer elements, reducing the overall complexity and cost. By optimizing the element positions within the sparse array, we can achieve comparable or even better performance than uniform arrays with fewer elements. This advantage makes sparse arrays an appealing choice for various applications, including radar systems and wireless communications.

Over the past few decades, numerous techniques have been developed for sparse array synthesis. As a conventional approach for sparse array synthesis, global optimization-based methodologies are used to find ideal sparse array configurations. These methods leverage stochastic approaches to locate optimal element spacings, encompassing techniques such as genetic algorithm [2], particle swarm optimization [3], and simulated annealing [4]. Notably, while these methods often yield effective results, they typically require significant computational time, which can be a limiting factor in practical applications.

In recent years, convex optimization techniques have become increasingly favored in the field of sparse array synthesis. These methods aim to optimize both antenna positions and their corresponding weights, with the goal of achieving a desired beampattern using the minimum number of elements within a given aperture. For instance, an iterative reweighted ℓ_1-norm minimization technique is proposed in [5] for synthesizing sparse arrays. Although it circumvents the intractability of the original ℓ_0-norm problem, it cannot guarantee obtaining the minimum number of antennas. As an improvement of the above algorithm, an efficient compressed-sensing inspired deterministic algorithm is presented in [6], incorporating a modified weighting function and a novel clustering technique. This approach avoids the situation where some antennas are too closely located, thereby improving performance in sparse array synthesis. In addition, a reconfigurable sparse array synthesis method is proposed in [7], using focal underdetermined system solver and multiple measurement vectors collaborative sparse recovery. Apart from the aforementioned work, there also exist other convex-optimization-based methods attempting to synthesize sparse arrays, as reported in [8], [9], and [10]. The convex-optimization-based sparse array synthesis methods mentioned above generally rely on selecting antennas from predefined grid points, which restricts the design freedom and flexibility. Although some off-grid methods have been attempted for sparse array synthesis recently [11], [12], they often require approximations and the solutions are complex.

In addition to the aforementioned methods, Oliveri and Massa [13] propose the use of sparse Bayesian learning (SBL) for sparse array synthesis. Given a reference beampattern, the algorithm models the deviation between the synthesized beampattern and the reference one. Ultimately, the sparse array synthesis problem is transformed into an SBL problem, which is then solved using relevance vector machines [14]. Separately, the matrix pencil method (MPM) is applied to sparse array synthesis in [15]. In the MPM-based method, the reference beampattern is sampled to construct a Hankel matrix. Based on the fact that the rank of Hankel matrix equals to the number of array elements, this method performs a low-rank approximation of the Hankel matrix to reduce element number and uses the inherent structure of matrix to determine the element position. Applications of MPM in various sparse array synthesis scenarios can be found in [16] and [17]. Using the continuous compressed sensing framework, Wang et al. [18] formulate sparse array synthesis as a sparse recovery problem. The problem is then tackled through semidefinite programming incorporating atomic norm minimization (ANM). The aforementioned sparse array synthesis methods based on SBL, MPM, and ANM require user-specified reference array and reference beampattern. However, different reference arrays/beampatterns can affect the performance of array synthesis, and currently there is a lack of theoretical basis for setting the optimal reference array/beampattern. In practical applications, it is desirable to conduct sparse array synthesis directly based on specific beampattern metrics, such as peak sidelobe level (PSL) and mainlobe width.

In this communication, we propose a sparse array synthesis method based on low-rank Hankel matrix completion [19]. Unlike the existing

work in [13], [14], [15], [16], [17], and [18], the proposed method does not require a user-specified reference array/beampattern. Based on the given metrics (e.g., PSL, mainlobe width) of the desired beampattern, we establish a sparse array synthesis model using low-rank Hankel matrix completion, which can be solved through log-det heuristic. The proposed model allows for the optimal design of desired values on beampattern, avoiding the issues of reference array/beampattern selection and potential performance degradation. In addition, our method can be easily extended to different scenarios of sparse array synthesis. Various examples (including numerical simulation and full-wave simulation) are presented to demonstrate the effectiveness and superiority of the proposed method. It is shown that the proposed method achieves more accurate estimation for element positions and synthesizes desired beampatterns with fewer antenna elements.

II. PRELIMINARIES

Assuming narrowband and far-field conditions, we consider a reference linear array with M elements. The reference beampattern can be expressed as

$$P(u) = \sum_{m=1}^{M} w_m E_m(u) e^{-j(2\pi/\lambda)p_m u} \qquad (1)$$

where $u \triangleq \sin(\theta)$ is the normalized spatial angle, and λ represents the wavelength. In (1), $E_m(u)$, p_m, and w_m denote the element pattern, position coordinate, and complex excitation coefficient of the mth antenna, respectively, $m = 1, \ldots, M$. We assume that the element patterns of all the antennas are identical, or they share a common average pattern $E(u)$. According to the pattern multiplication principle [20], we can then express the reference beampattern $P(u)$ as

$$P(u) = E(u) F(u). \qquad (2)$$

In (2), $F(u)$ is the reference array factor, which can be calculated as

$$F(u) = \mathbf{w}_r^{\mathrm{T}} \mathbf{a}_r(u) \qquad (3)$$

where $(\cdot)^{\mathrm{T}}$ represents the transpose operation, $\mathbf{a}_r(u) = [e^{-j(2\pi/\lambda)p_1 u}, \ldots, e^{-j(2\pi/\lambda)p_M u}]^{\mathrm{T}}$ stands for the steering vector of the reference array, and $\mathbf{w}_r = [w_1, \ldots, w_M]^{\mathrm{T}}$ is the complex excitation vector, which can be preset according to the desired beampattern characteristics. According to (2), we can perform array design by focusing solely on the array factor $F(u)$, which typically takes complex values.

To achieve sparse array synthesis, the MPM-based method [15] approximates the array factor $F(u)$ using as few antennas as possible. To this end, the array factor $F(u)$ is sampled uniformly to obtain the data v_k

$$v_k = F(u)|_{u=k\Delta}, \quad k = -K, \ -K+1, \ldots, K \qquad (4)$$

where Δ represents the sampling interval, and the sample number is $2K+1$. Constructing the following $(2K-L+2) \times L$ Hankel matrix with coefficients $v_{-K}, \ldots, v_K$:

$$\mathbf{Y}(v_{-K}, \ldots, v_K) \triangleq \begin{bmatrix} v_{-K} & v_{-K+1} & \cdots & v_{-K+L-1} \\ v_{-K+1} & v_{-K+2} & \cdots & v_{-K+L} \\ \vdots & \vdots & \ddots & \vdots \\ v_{K-L+1} & v_{K-L+2} & \cdots & v_K \end{bmatrix}$$

where L is the matrix pencil parameter, and it can be further derived that

$$\mathrm{rank}(\mathbf{Y}) = M. \qquad (5)$$

Based on (5), the MPM-based method performs a low-rank approximation of the matrix $\mathbf{Y}$ to reduce the number of antenna elements.

It should be noted that the aforementioned approach relies on a user-specified reference array/beampattern. However, there is
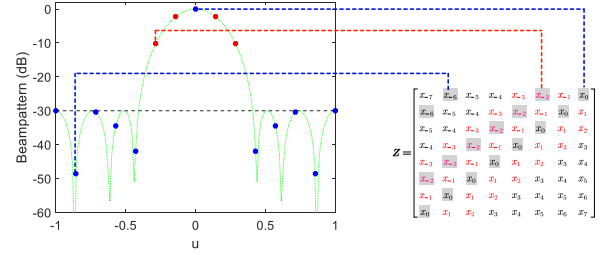
Fig. 1. Schematic of the proposed method.

currently no theoretical basis for determining the optimal reference array/beampattern according to the given beampattern metrics. Next, we propose a sparse array synthesis method using low-rank Hankel matrix completion, which eliminates the need for setting reference array and reference beampattern.

III. SPARSE ARRAY SYNTHESIS USING LOW-RANK HANKEL MATRIX COMPLETION

In this section, we first formulate the low-rank Hankel matrix completion model for sparse array synthesis. On this basis, a log-det heuristic algorithm is presented to solve the low-rank Hankel matrix completion problem. Finally, we discuss the extensions of the proposed method in various sparse array synthesis scenarios. For simplicity, we assume that the antennas are isotropic.

A. Formulation of Low-Rank Hankel Matrix Completion

We take the sparse array synthesis of focused beam as an example. For the sake of clarity and ease of explanation, Fig. 1 presents a schematic of the proposed method. Let u_0 be the mainlobe axis, the normalized upper sidelobe level at spatial angle u is $\rho(u)$. According to the beampattern metrics, we can obtain the mainlobe region Ψ_m and the sidelobe region Ψ_s. Unlike the existing methods that construct the Hankel matrix by sampling the reference beampattern, we directly design a low-rank Hankel matrix while satisfying the beampattern constraints.

More specifically, we take $u_0 = 0$ as an example and assume that the Hankel matrix $\mathbf{Z}$ consists of coefficients $x_{-K}, \ldots, x_K$, where x_k's represent the beampattern data that we need to determine. The angle interval corresponding to x_k and x_{k+1} is Δ, as mentioned in (4) and depicted in Fig. 1. Based on the given Ψ_m, Ψ_s, and Δ, we can define the following sets of indices describing the mainlobe and sidelobe with respect to the points x_k:

$$\mathbb{M} \triangleq \{-S+1, \ldots, S-1\} \qquad (6)$$
$$\mathbb{S} \triangleq \{-K, \ldots, -S, S, \ldots, K\} \qquad (7)$$

where S corresponds to the index of sidelobe boundary. Then, x_m corresponds to a point in the mainlobe of the beampattern if $m \in \mathbb{M}$, and x_s belongs to a point in the sidelobe of the beampattern if $s \in \mathbb{S}$.

To achieve a focused beam, we constrain the point x_0 on the mainlobe axis to be a positive constant η and constrain the point x_s in the sidelobe region to have a lower modulus than the desired level $\eta \cdot \rho(s\Delta)$, where $s \in \mathbb{S}$. Based on these constraints, we can minimize the number of array elements by minimizing the rank of the aforementioned Hankel matrix $\mathbf{Z}$. Thus, we obtain the following low-rank Hankel matrix completion formulation for sparse array synthesis:

$$\min_{\mathbf{Z}} \ \mathrm{rank}\left[\mathbf{Z}(x_{-K}, \ldots, x_K)\right] \qquad (8a)$$
$$\text{s.t. } x_0 = \eta \qquad (8b)$$
$$|x_s| \leq \eta \cdot \rho(s\Delta), \quad s \in \mathbb{S} \qquad (8c)$$
$$\mathbf{Z}(x_{-K}, \ldots, x_K) \in \mathbb{H}^{(2K-L+2) \times L} \qquad (8d)$$

where $\mathbb{H}$ denotes the set of Hankel matrices with dimensions specified by the superscript. It should be noted that the variables x_k's in (8) can be complex-valued. Based on the given metrics on the desired beampattern, the formulation (8) recovers the uncertain and incomplete Hankel matrix Z while satisfying specified beampattern constraints.

B. Solving Problem (8) Using Log-Det Heuristic

Note that the matrix Z is complex-valued and not necessarily square, which indicates that problem (8) typically does not have an analytical solution. In fact, according to the semidefinite embedding lemma in [21], we can convert problem (8) into a task of minimizing the rank of a block-diagonal semidefinite matrix. More specifically, by introducing Hermitian matrices P and T, the problem (8) can be equivalently expressed as

$$\min_{Z,P,T} \frac{1}{2} \text{rank} \left[\text{diag}\left(P,T\right) \right] \tag{9a}$$

$$\text{s.t.} \begin{bmatrix} P & Z \\ Z^H & T \end{bmatrix} \succeq 0 \tag{9b}$$

$$x_0 = \eta \tag{9c}$$

$$|x_s| \le \eta \cdot \rho\left(s\Delta\right), \quad s \in \mathbb{S} \tag{9d}$$

$$Z\left(x_{-K}, \ldots, x_K\right) \in \mathbb{H}^{(2K-L+2) \times L} \tag{9e}$$

where $\text{diag}(P,T)$ is a block diagonal matrix given by

$$\text{diag}\left(P,T\right) \triangleq \begin{bmatrix} P & 0 \\ 0 & T. \end{bmatrix} \tag{10}$$

In this communication, we use the log-det heuristic [21] to solve the above problem (9). Since $\text{diag}(P,T)$ is semidefinite, the function $\log \det[\text{diag}(P,T) + \delta I]$ can be seen as a smooth surrogate for rank $[\text{diag}(P,T)]$, where $\delta > 0$ is a small regularization constant. Instead of solving (9), we consider the following problem:

$$\min_{Z,P,T} \log \det \left[\text{diag}\left(P,T\right) + \delta I \right] \tag{11a}$$

$$\text{s.t.} \begin{bmatrix} P & Z \\ Z^H & T \end{bmatrix} \succeq 0 \tag{11b}$$

$$x_0 = \eta \tag{11c}$$

$$|x_s| \le \eta \cdot \rho\left(s\Delta\right), \quad s \in \mathbb{S} \tag{11d}$$

$$Z\left(x_{-K}, \ldots, x_K\right) \in \mathbb{H}^{(2K-L+2) \times L}. \tag{11e}$$

Note that in the above problem, all the constraints are convex, whereas the objective function (11a) is nonconvex.

Based on the analysis presented in [21], we use iterative linearization to find a local minimum for the above problem (11). This leads to the following iterations for solving (11) locally:

$$\min_{Z,P,T} \text{Tr} \left[V_i \text{diag}\left(P,T\right) \right] \tag{12a}$$

$$\text{s.t.} \begin{bmatrix} P & Z \\ Z^H & T \end{bmatrix} \succeq 0 \tag{12b}$$

$$x_0 = \eta \tag{12c}$$

$$|x_s| \le \eta \cdot \rho\left(s\Delta\right), \quad s \in \mathbb{S} \tag{12d}$$

$$Z\left(x_{-K}, \ldots, x_K\right) \in \mathbb{H}^{(2K-L+2) \times L} \tag{12e}$$

where $V_i \triangleq [\text{diag}(P_{i-1},T_{i-1}) + \delta I]^{-1}$ represents the weight matrix in the ith iteration, and the matrices P_{i-1} and T_{i-1} are solved from the $(i-1)$th iteration. In the first iteration, we can initially choose $V_1 = I$. The iteration process terminates when rank(Z) remains unchanged over multiple consecutive iterations. Note that the problem (12) is a convex program, which can be solved using off-the-shelf solver, such as cvx [22]. Moreover, as discussed in [21], the trace function [refer to (12a)] acts as the convex envelope of the rank function for matrices with norm less than one. This provides a

theoretical support for using the trace heuristic in our approach. Due to the local solving nature, we cannot guarantee that the sequential solutions to (12) converge to the global optimum of the low-rank Hankel matrix completion problem (8). Nevertheless, our simulation results indicate that the algorithm converges after a limited number of iterations and produces satisfactory low-rank solutions.

Remark: In the above formulations, no constraints are imposed on points within the mainlobe region apart from x_0. However, simulations have discovered that the application of log-det heuristic in this scenario may yield a trivial solution, where x_0 equals η and all other values are zero. To obtain a nontrivial solution, it is necessary to select a few additional points x_l's (usually two or three are sufficient) within the mainlobe region and impose the following convex constraint:

$$|x_l - \eta| \le |\eta| - \alpha \tag{13}$$

where α is a positive constant satisfying $\alpha \ll |\eta|$. It is not difficult to find that the constraint (13) can avoid the occurrence of $x_l = 0$.

C. Determination of Antenna Position and Excitation

After obtaining the low-rank Hankel matrix Z, the antenna locations and excitation vectors can be determined based on MPM [15]. Specifically, assuming rank(Z) = R, the positions of the rth antenna in the sparse array can be obtained by

$$\hat{p}_r = \frac{\lambda \cdot \ln\left(\beta_r\right)}{j 2\pi \Delta}, \quad r = 1, \ldots, R \tag{14}$$

where $j \triangleq \sqrt{-1}$, β_r represents the rth eigenvalue of matrix $Z_1^\dagger Z_2$, and Z_1 and Z_2 represent the matrices obtained by deleting the first column and last column from Z, respectively. Unlike the MPM-based method, the proposed method does not require an additional low-rank approximation step. It ensures that the matrix Z, which retains its Hankel structure, can be directly used for estimating the array element positions, thereby achieving more accurate estimation results.

Based on the relationship between the beampattern data x_k and the excitation vector w, it is not difficult to obtain the following equation:

$$\underbrace{\begin{bmatrix} \beta_1^{-K} & \beta_2^{-K} & \cdots & \beta_R^{-K} \\ \beta_1^{-K+1} & \beta_2^{-K+1} & \cdots & \beta_R^{-K+1} \\ \vdots & \vdots & \ddots & \vdots \\ \beta_1^K & \beta_2^K & \cdots & \beta_R^K \end{bmatrix}}_{A} \underbrace{\begin{bmatrix} \omega_1 \\ \omega_2 \\ \vdots \\ \omega_R \end{bmatrix}}_{w} = \underbrace{\begin{bmatrix} x_{-K} \\ x_{-K+1} \\ \vdots \\ x_K \end{bmatrix}}_{x}.$$

In the least-squares sense, the following estimate for the excitation vector can be obtained:

$$\hat{w} = \left(A^H A\right)^{-1} A^H x. \tag{15}$$

Finally, the array factor for the synthesized sparse array can be expressed as

$$f(u) = \hat{w}^T a(u) \tag{16}$$

where $a(u)$ represents the steering vector of the resulting sparse array.

D. Extensions of the Proposed Method

The proposed sparse array synthesis scheme can be easily extended to more complex scenarios. Next, we consider two extensions of the proposed method. The first extension is sparse linear array synthesis with a shaped beampattern as desired. The second one is to synthesize a sparse linear array with multiple beampatterns.

1) Sparse Linear Array Synthesis With a Shaped Beampattern: For shaped beampattern, it is typically necessary to design the beam according to a specific shape, primarily in the mainlobe region. In this case, we can incorporate the beam constraints into low-rank Hankel
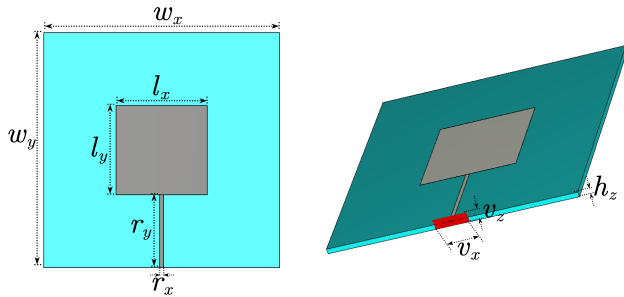
Fig. 2. Illustration of the patch antenna element.

Fig. 3. Result of the proposed method with a focused beam. (a) Beampattern result. (b) Curve of rank($\mathbf{Z}$) versus iteration step.

matrix completion. More specifically, we can impose the following constraint:

$$|x_m - \gamma(m\Delta)| \leq \xi, \quad m \in \bar{\mathbb{M}} \tag{17}$$

where $\gamma(m\Delta)$ is preassigned and gives the desired shaped beampattern level at spatial angle $m\Delta$, ξ is a given threshold, and $\bar{\mathbb{M}}$ represents the set of spatial angles used for shaped beampattern constraints. Note that the above constraint (17) is convex.

2) Sparse Linear Array Synthesis With Multiple Beampatterns: In the second scenario, we expect to synthesize a reconfigurable sparse array that can radiate multiple distinct radiation beampatterns by varying the element excitations. Following the model for multi-beampattern sparse array synthesis presented in [17], we can directly design the following low-rank block Hankel matrix:

$$\mathbf{\Xi} = \begin{bmatrix} \mathbf{Z}\left(x_{-K}^{(1)}, \ldots, x_K^{(1)}\right) \\ \mathbf{Z}\left(x_{-K}^{(2)}, \ldots, x_K^{(2)}\right) \\ \vdots \\ \mathbf{Z}\left(x_{-K}^{(Q)}, \ldots, x_K^{(Q)}\right) \end{bmatrix} \tag{18}$$

where Q represents the number of synthesized beampatterns, $x_k^{(q)}$ denotes the beampattern data at spatial angle $k\Delta$, and for the qth beampattern, $k = -K, \ldots, K$, $q = 1, \ldots, Q$. By imposing constraints on $x_k^{(q)}$ according to the desired beampattern metrics, we can formulate a low-rank matrix completion model to minimize the rank of block Hankel matrix $\mathbf{\Xi}$. This allows us to recover the multiple beampattern data automatically while ensuring the minimum antenna number.

IV. SIMULATION

In this section, we conduct representative simulations to demonstrate the efficacy and advantage of the proposed method.[1] To evaluate performance of our method, we benchmark it against the MPM method in [15] and the ANM method in [18]. To see the impact of mutual coupling on the proposed method, we conduct full-wave simulations with patch antennas using CST full-wave simulation software, operating at a center frequency of 2.5 GHz. The dielectric permittivity of the substrate is $\epsilon_r = 2.2$. Other topological details of the patch antenna element can be found in Fig. 2, where $w_x = w_y = 100$, $l_x = 38$, $l_y = 38.6$, $r_x = 1.46$, $r_y = 30.7$, $v_x = 13.46$, $v_z = 8.035$, and $h_z = 2$, all units are in millimeters.

A. Sparse Array Synthesis With a Focused Beampattern

In the first example, we consider sparse array synthesis for a focused beampattern with equal sidelobe level. The beam is pointed toward the normal direction of the array. For MPM and ANM methods, we use the Chebyshev beampattern of a ULA with 20 elements

[1]The MATLAB codes for the proposed method are available online at https://zhangxuejing7.github.io/HomePage/
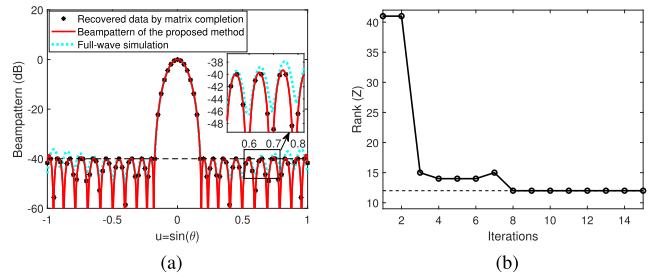
TABLE I
RESULTS OF ELEMENT POSITIONS AND EXCITATIONS FOR FOCUSED BEAM SPARSE ARRAY SYNTHESIS

r	$\hat{p}_r/\lambda$	$\hat{w}_r$	r	$\hat{p}_r/\lambda$	$\hat{w}_r$	r	$\hat{p}_r/\lambda$	$\hat{w}_r$
1	0	0.198	5	3.368	1.476	9	6.730	1.153
2	0.844	0.433	6	4.208	1.664	10	7.572	0.776
3	1.685	0.776	7	5.049	1.664	11	8.413	0.433
4	2.527	1.153	8	5.889	1.476	12	9.257	0.198

as reference. For the proposed method, we set $K = 40$, $L = 41$, $\eta = 13$, $\alpha = 1$, and $\delta = 0.1$.

1) Performance Demonstration and Comparison: We assume that the desired PSL is -40 dB, and the mainlobe width is equal to that of a Chebyshev beampattern. The result of the proposed method is presented in Fig. 3. Fig. 3(a) illustrates the recovered beampattern data x_k using the proposed method, as well as the ultimate beampattern and full-wave simulation result. As can be seen from Fig. 3(a), the data recovered using low-rank Hankel matrix completion meet the given radiation requirements. Meanwhile, the radiation beampattern and full-wave simulation result are satisfactory. Fig. 3(b) depicts the curve of rank($\mathbf{Z}$) versus iteration step. It can be observed that rank($\mathbf{Z}$) gradually decreases and tends to converge after eight iterations, ultimately resulting in rank($\mathbf{Z}$) = 12. Accordingly, the number of sparse array elements obtained by the proposed method is 12. Table I provides detailed results of ultimate element positions and excitations, where the array has been normalized to the origin.

Fig. 4 shows comparison of the performance of different methods. The beampatterns obtained by different methods are depicted in Fig. 4(a). It should be noted that for a fair comparison, the element number is set to 12 for MPM and ANM methods. With the same number of elements, the proposed method achieves lower PSL. Considering that all three methods estimate element positions based on the matrix pencil principle, Fig. 4(b) presents the distribution of eigenvalues (see (11) in [15] and (16) in [18]) in the complex plane during the estimation of element positions. As evident from Fig. 4(b), the eigenvalues of the proposed method are closer to the unit circle in the complex plane, indicating a more accurate element position estimation result. Finally, the sparse array distributions of different methods are compared in Fig. 4(c).

2) Performance of the Proposed Method Under Different PSLs and Mainlobe Widths: To demonstrate the flexibility and effectiveness of the proposed method, its performance is evaluated under different beampattern metrics. In the first case, the PSL is set to -28, -36, and -44 dB, respectively. Fig. 5(a) illustrates the beampatterns obtained by the proposed method for the above three PSLs. It is evident that the proposed algorithm can achieve satisfactory beampattern results based on the desired PSL metrics. To assess the impact of PSL on the resulting number of elements in the sparse array, Fig. 5(b) depicts the curve of obtained element number versus PSL. It is clear that as PSL increases, the number of required elements decreases.
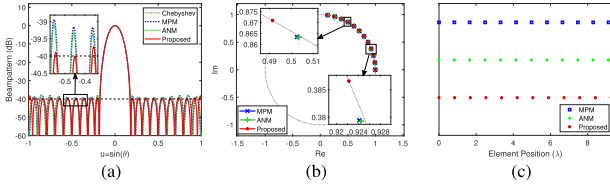
Fig. 4. Performance comparison of different methods for focused-beam sparse array synthesis. (a) Beampattern comparison. (b) Comparison of eigenvalue distribution in the complex plane. (c) Comparison of sparse array distributions.
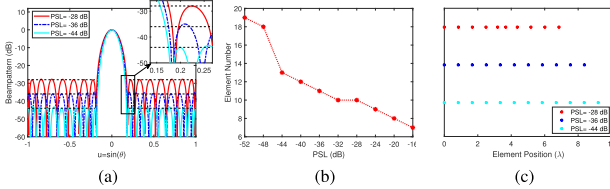
Fig. 5. Performance illustration of the proposed method with different PSLs. (a) Beampattern results. (b) Curve of obtained element number versus PSL. (c) Obtained sparse array distributions.
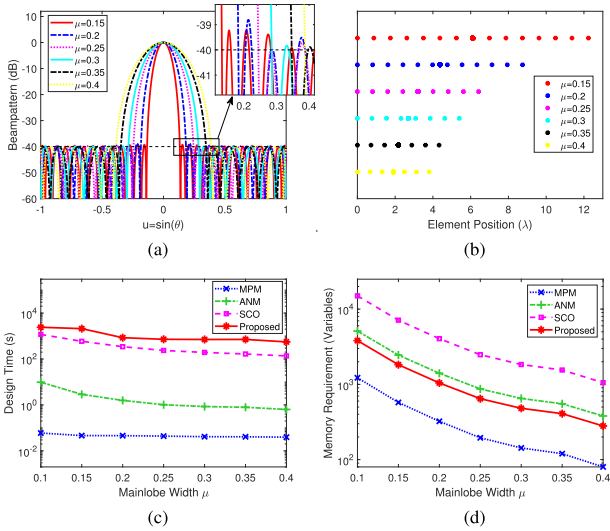
Fig. 6. Simulation results with different mainlobe width configurations. (a) Beampattern results of the proposed algorithm. (b) Obtained sparse array distributions of the proposed algorithm. (c) Design time comparison of different algorithms. (d) Memory usage comparison of different algorithms.

Fig. 5(c) shows the sparse array distributions under different PSLs.

In the second scenario, we set the desired PSL as -40 dB and evaluate the performance of the proposed method under different mainlobe width configurations. The simulation results with different mainlobe width configurations are presented in Fig. 6, where the parameter μ is defined as half of the width between the first nulls of mainlobe. Fig. 6(a) shows the beampatterns obtained by the proposed method for various mainlobe widths, and Fig. 6(b) presents the corresponding sparse array distributions. From Fig. 6(a), it is evident that the proposed method can achieve satisfactory beampattern results under different mainlobe widths. In addition, Fig. 6(b) reveals that a wider mainlobe width requires fewer array elements. To further assess the complexity of the proposed method, Fig. 6(c) and (d) shows comparison of the design times and required memory (here approximated by the number of variables) of different algorithms under varying mainlobe widths, with the sequential convex optimization (SCO) method in [5] also considered. The simulation results reveal that as the mainlobe width is set narrower, the design time of each algorithm increases, and more memory/variables are needed. Due to the iterative solution process, the design time of the proposed
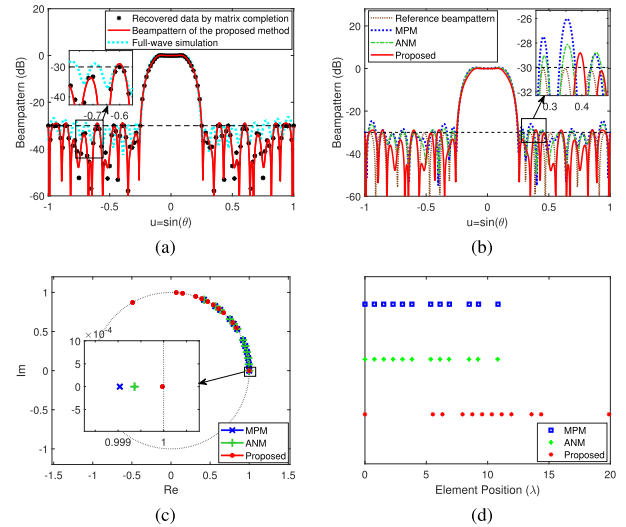
Fig. 7. Performance comparison of different methods for shaped beam sparse array synthesis. (a) Beampattern result of the proposed method. (b) Beampattern comparison of different algorithms. (c) Comparison of eigenvalue distribution in the complex plane. (d) Comparison of sparse array distributions.

TABLE II

RESULTS OF ELEMENT POSITIONS AND EXCITATIONS FOR SHAPED BEAM SPARSE ARRAY SYNTHESIS

r	$\hat{p}_r/\lambda$	$\hat{w}_r$	r	$\hat{p}_r/\lambda$	$\hat{w}_r$	r	$\hat{p}_r/\lambda$	$\hat{w}_r$
1	0	0.167	5	8.747	5.106	9	11.935	2.218
2	5.532	-0.711	6	9.548	7.090	10	13.577	-0.992
3	6.314	-0.992	7	10.343	7.090	11	14.359	-0.711
4	7.956	2.218	8	11.144	5.106	12	19.891	0.167

method is longer than that of the other three methods. In terms of memory usage, the proposed method only exceeds the MPM method but is lower than the ANM and SCO methods.

B. Sparse Array Synthesis With a Shaped Beampattern

To assess the performance of the proposed algorithm in sparse array synthesis for shaped beampatterns, we consider a flat-top-shaped beampattern scenario. We set the PSL to -30 dB and specify a flat-top mainlobe width of $11.5°$. We use the method in [23] to generate the reference beampattern for MPM and ANM. The reference linear array has 30 elements with a spacing of $0.5\ \lambda$.

Fig. 7 presents the sparse array synthesis results. Fig. 7(a) illustrates the beampattern data recovered using our method and the full-wave simulation result, demonstrating that the resulting beampattern meets the expected requirements. In this case, our method obtains 12 array elements after ten iteration steps. With the array element number fixed at 12 for MPM and ANM, Fig. 7(b) shows comparison of the beampattern results of different methods. We can see that the proposed method achieves a flatter mainlobe beam and lower PSL when compared with MPM and ANM. Fig. 7(c) shows comparison of the eigenvalue distributions of the three methods. It can be seen that the eigenvalues of our method are closer to the unit circle, indicating a more precise element position estimation. The sparse array distributions resulting from the three methods are presented in Fig. 7(d). Table II provides detailed information on the ultimate element positions and excitations obtained through the proposed method.

C. Sparse Array Synthesis With Multiple Beampatterns

To demonstrate the broad applicability of the proposed scheme, we assess the performance of sparse array synthesis for multiple
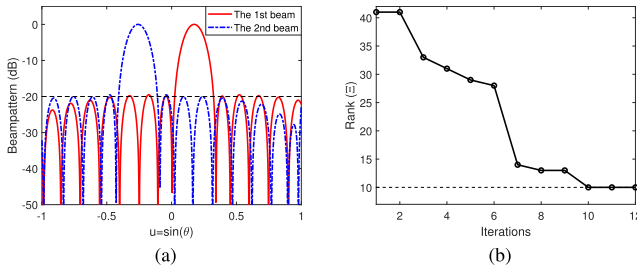
Fig. 8. Performance illustration of the proposed method with multiple-beam sparse array synthesis. (a) Beampattern result. (b) Curve of rank(Ξ) versus iteration step.

TABLE III
RESULTS OF ELEMENT POSITIONS AND EXCITATIONS FOR
MULTIPLE-BEAM SPARSE ARRAY SYNTHESIS

r	$\hat{p}_r/\lambda$	$\hat{w}_r^{(1)}$	$\hat{w}_r^{(2)}$
1	0	$0.078e^{-j2.869}$	$0.076e^{+j1.195}$
2	0.653	$0.076e^{+j2.702}$	$0.076e^{+j2.257}$
3	1.363	$0.099e^{+j1.927}$	$0.100e^{-j2.872}$
4	2.069	$0.119e^{+j1.157}$	$0.119e^{-j1.724}$
5	2.776	$0.130e^{+j0.385}$	$0.128e^{-j0.574}$
6	3.482	$0.130e^{-j0.385}$	$0.128e^{+j0.574}$
7	4.189	$0.119e^{-j1.157}$	$0.119e^{+j1.724}$
8	4.895	$0.099e^{-j1.927}$	$0.100e^{+j2.872}$
9	5.605	$0.076e^{-j2.702}$	$0.076e^{-j2.257}$
10	6.258	$0.078e^{-j2.869}$	$0.076e^{-j1.195}$

beampatterns. For simplicity, we consider two focused beampatterns, with beam directions pointing to $10°$ ($\sin(10°) \approx 0.174$) and $-15°$ ($\sin(-15°) \approx -0.259$), respectively. The PSL is -20 dB. In this case, we design a low-rank block Hankel matrix Ξ in (18) under beampattern constraints.

Fig. 8(a) illustrates the two beampatterns obtained using the proposed method. It is evident that both the beampatterns meet the desired radiation performance. Fig. 8(b) depicts the change in rank(Ξ) with iterations. We can see that the proposed method tends to converge after ten iterations, resulting in a matrix Ξ with a rank of 10. Table III presents the final element positions and the corresponding excitations for the two beams. The results clearly demonstrate the versatility and effectiveness of our proposed scheme in synthesizing sparse arrays for multiple beampatterns.

V. CONCLUSION

In this communication, we have presented a method for synthesizing sparse linear arrays using low-rank Hankel matrix completion. Our method generates the sparse linear array based on the desired beampattern metrics (such as PSL and mainlobe width), without using reference array/beampattern. We formulate the sparse array synthesis problem as a low-rank matrix completion task and solve it using log-det heuristic. By preserving the Hankel structure, our method has demonstrated superior accuracy in estimating element positions. Compared with existing works, our method offers superior flexibility and can generate the desired beampatterns using fewer antenna elements, although it has the drawback of long computational time. In addition, the proposed method is suitable for diverse sparse array synthesis scenarios across different applications, including short-range communication [24] and radar sensing. In such applications, our method could potentially contribute to enhancing performance metrics such as directivity and signal-to-noise ratio.

REFERENCES

[1] M. D'Urso, G. Prisco, and R. M. Tumolo, "Maximally sparse, steerable, and nonsuperdirective array antennas via convex optimizations," *IEEE Trans. Antennas Propag.*, vol. 64, no. 9, pp. 3840–3849, Sep. 2016.

[2] K.-K. Yan and Y. Lu, "Sidelobe reduction in array-pattern synthesis using genetic algorithm," *IEEE Trans. Antennas Propag.*, vol. 45, no. 7, pp. 1117–1122, Jul. 1997.

[3] D. W. Boeringer and D. H. Werner, "Particle swarm optimization versus genetic algorithms for phased array synthesis," *IEEE Trans. Antennas Propag.*, vol. 52, no. 3, pp. 771–779, Mar. 2004.

[4] V. Murino, A. Trucco, and C. S. Regazzoni, "Synthesis of unequally spaced arrays by simulated annealing," *IEEE Trans. Signal Process.*, vol. 44, no. 1, pp. 119–122, Jan. 1996.

[5] B. Fuchs, "Synthesis of sparse arrays with focused or shaped beampattern via sequential convex optimizations," *IEEE Trans. Antennas Propag.*, vol. 60, no. 7, pp. 3499–3503, Jul. 2012.

[6] D. Pinchera, M. D. Migliore, F. Schettino, M. Lucido, and G. Panariello, "An effective compressed-sensing inspired deterministic algorithm for sparse array synthesis," *IEEE Trans. Antennas Propag.*, vol. 66, no. 1, pp. 149–159, Jan. 2018.

[7] F. Yan, P. Yang, F. Yang, L. Zhou, and M. Gao, "Synthesis of pattern reconfigurable sparse arrays with multiple measurement vectors FOCUSS method," *IEEE Trans. Antennas Propag.*, vol. 65, no. 2, pp. 602–611, Feb. 2017.

[8] B. Fuchs, "Application of convex relaxation to array synthesis problems," *IEEE Trans. Antennas Propag.*, vol. 62, no. 2, pp. 634–640, Feb. 2014.

[9] F. Yang et al., "Synthesis of irregular phased arrays subject to constraint on directivity via convex optimization," *IEEE Trans. Antennas Propag.*, vol. 69, no. 7, pp. 4235–4240, Jul. 2021.

[10] B. Fuchs and S. Rondineau, "Array pattern synthesis with excitation control via norm minimization," *IEEE Trans. Antennas Propag.*, vol. 64, no. 10, pp. 4228–4234, Oct. 2016.

[11] S. Yang, B. Liu, Z. Hong, and Z. Zhang, "Low-complexity sparse array synthesis based on off-grid compressive sensing," *IEEE Antennas Wireless Propag. Lett.*, vol. 21, no. 12, pp. 2322–2326, Dec. 2022.

[12] M. A. Abdelhay, N. O. Korany, and S. E. El-Khamy, "Synthesis of uniformly weighted sparse concentric ring arrays based on off-grid compressive sensing framework," *IEEE Antennas Wireless Propag. Lett.*, vol. 20, no. 4, pp. 448–452, Apr. 2021.

[13] G. Oliveri and A. Massa, "Bayesian compressive sampling for pattern synthesis with maximally sparse non-uniform linear arrays," *IEEE Trans. Antennas Propag.*, vol. 59, no. 2, pp. 467–481, Feb. 2011.

[14] G. Oliveri, M. Carlin, and A. Massa, "Complex-weight sparse linear array synthesis by Bayesian compressive sampling," *IEEE Trans. Antennas Propag.*, vol. 60, no. 5, pp. 2309–2326, May 2012.

[15] Y. Liu, Z. Nie, and Q. H. Liu, "Reducing the number of elements in a linear antenna array by the matrix pencil method," *IEEE Trans. Antennas Propag.*, vol. 56, no. 9, pp. 2955–2962, Sep. 2008.

[16] Y. Liu, Q. H. Liu, and Z. Nie, "Reducing the number of elements in the synthesis of shaped-beam patterns by the forward-backward matrix pencil method," *IEEE Trans. Antennas Propag.*, vol. 58, no. 2, pp. 604–608, Feb. 2010.

[17] Y. Liu, Q. H. Liu, and Z. Nie, "Reducing the number of elements in multiple-pattern linear arrays by the extended matrix pencil methods," *IEEE Trans. Antennas Propag.*, vol. 62, no. 2, pp. 652–660, Feb. 2014.

[18] Z. Wang, G. Sun, J. Tong, and Y. Ji, "Pattern synthesis for sparse linear arrays via atomic norm minimization," *IEEE Antennas Wireless Propag. Lett.*, vol. 20, no. 12, pp. 2215–2219, Dec. 2021.

[19] X. Zhang, "Synthesis of sparse linear arrays via low-rank Hankel matrix completion," 2022, *arXiv:2209.04577.*

[20] P. Rocca, G. Oliveri, R. J. Mailloux, and A. Massa, "Unconventional phased array architectures and design methodologies—A review," *Proc. IEEE*, vol. 104, no. 3, pp. 544–560, Mar. 2016.

[21] M. Fazel, H. Hindi, and S. P. Boyd, "Log-det heuristic for matrix rank minimization with applications to Hankel and Euclidean distance matrices," in *Proc. Amer. Control Conf.*, vol. 3, Jun. 2003, pp. 2156–2162.

[22] M. Grant and S. Boyd. (2015). *CVX: MATLAB Software for Disciplined Convex Programming, Version 2.1.* [Online]. Available: http://cvxr.com/cvx

[23] X. Zhang, Z. He, B. Liao, X. Zhang, and W. Peng, "Pattern synthesis for arbitrary arrays via weight vector orthogonal decomposition," *IEEE Trans. Signal Process.*, vol. 66, no. 5, pp. 1286–1299, Mar. 2018.

[24] O. Leonardi, M. G. Pavone, G. Sorbello, A. F. Morabito, and T. Isernia, "Compact single-layer circularly polarized antenna for short-range communication systems," *Microw. Opt. Technol. Lett.*, vol. 56, no. 8, pp. 1843–1846, Aug. 2014.